

Flexible Strain Gauge Sensors as Real-time Stretch Receptors for Use in Biomimetic BPA Muscle Applications

Rochelle Jubert¹, Alexander Hunt¹, and Michael Hopkins²

¹Department of Mechanical and Materials Engineering, Portland State University,
Portland, OR, USA

²Liquid Wire, Portland, OR, USA

Abstract. This paper presents a novel approach to real-time length sensing for biomimetic Braided Pneumatic Actuators (BPAs) in soft robotics applications. Flexible strain gauge sensors from LiquidWire are ironed onto a sewn Nylon sleeve for external placement on BPAs. Calibration equations that include voltage rate and hysteresis are developed to convert strain gauge resistance into muscle displacement. Experimental results demonstrate the efficacy of the proposed method, achieving low error rates and high biomimicry. The non-linear calibration outperforms linear methods, showcasing its suitability for artificial proprioceptive neural networks. This approach offers accurate real-time feedback for enhanced robotic control, addressing the need for low-profile, modular sensors that mimic muscle stretch receptors. Future research may explore further refinements and applications of this technique.

1 Introduction

Artificial muscles, such as braided pneumatic actuators (BPAs), are frequently used to develop biomimetic robots due to their muscle-like properties [?, ?, ?, ?]. These actuators provide variable stiffness and often exhibit similar force-length and force-velocity dependencies that are found in biological muscles. The use of artificial muscles enables the development of more interesting robotic designs that no longer depend on single rotation joints controlled by motors; other joint designs, such as ball-and-socket and compact, four-bar mechanisms can be created [?, ?]. Additionally, artificial muscles can be arranged in complex geometries and cross multiple joints. Developing robots with these capabilities, however, produces more complexities in control and sensing. Joint encoders, the mainstay of robotic feedback, can no longer be used. New methods of sensing are needed to get feedback on muscle behavior to implement intelligent controls.

Here again, we can take inspiration from how biological systems provide sensory feedback of muscle movement and contraction in the body. Animals sense movement in their bodies through proprioceptive feedback [?]. These sensory neurons include spindles and stretch receptors that are wrapped around and embedded in muscle and tendon tissues [10]. They are known to sense muscle

velocity, tension, and length, also referred to as Types Ia, Ib, and II. This feedback is then integrated into the nervous system and used for control of individual muscles, and coordination of muscle groups [8]. The development of sensors that mimic this feedback could significantly improve the controllability of artificial muscles.

Several methods have been explored to incorporate real-time length sensing abilities into BPA design, aiming to mimic the function of muscle stretch receptors and complete the artificial proprioceptive feedback loop. This can be achieved by weaving sensors within the fabric of the BPA, placing sensors inside, or by attaching sensors externally. While structural sensors that are integrated directly into the fabric provide a low-profile and biomimetic solution, the muscle fabrication processes are labor-intensive and inaccessible to research being conducted with stock BPAs [5, 12, 13]. Sensors that are placed inside of the BPA bladder produce a low-profile design, however, these methods suffer from poor noise-to-signal ratios, making them less suitable for precise soft robotic control [1,3,6]. Therefore, the use of flexible external sensors made from piezoelectric materials such as Gallium-Indium or ElectroLycra has been increasing due to their modularity, biomimetic characteristics, and low-profile application methods [4, 9]. Although these methods have developed some clever techniques for capturing strain rate and hysteresis, they experience some challenges with noise and material choice such that they are unable to produce length measurements at a high enough accuracy that would be useful for feedback control.

This research sets out to fill this gap by developing a reliable method for sensing artificial muscle length for use as feedback in a BPA-actuated robot. Similar to previous research [9], we consider strain rate and hysteresis when generating calibration equations to convert the strain gauge resistance to muscle length. We test this calibration against both slow motions and fast motions that replicate signals that may be sent to the robot during locomotion. We demonstrate that the proposed design, signal processing, and calibration provide a promising method for producing precise muscle-length sensing ability that is biomimetic, low-profile, modular, and suitable as feedback in artificial robotic proprioceptive control.

2 Methods

To collect consistent real-time length data while minimizing noise, a sturdy length-sensing test rig was built, as seen in Figure 1.

The extruded aluminum frame held a sliding crossbeam that displaced as an attached 180 cm long, 10mm diameter stock Festo BPA was inflated and deflated with two respective orientations of valves, as seen in Figure 2—one inflation orientation with a Kelly Pneumatics Miniature Proportional valve upstream of a 3/2 way AirTAC solenoid valve to modulate muscle inflation and one deflation orientation with the proportional valve downstream of the binary solenoid valve to modulate deflation. These two configurations allowed for more precise control

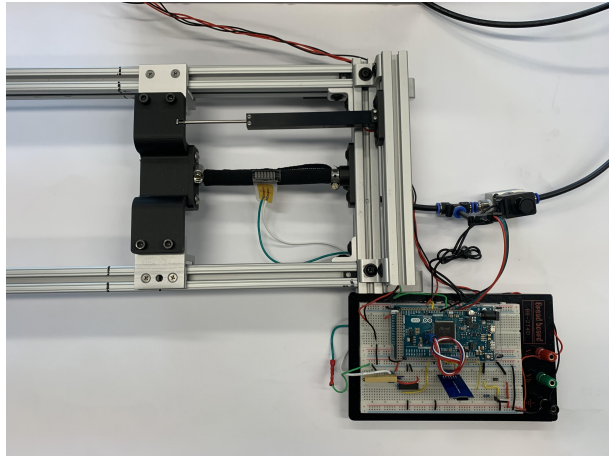
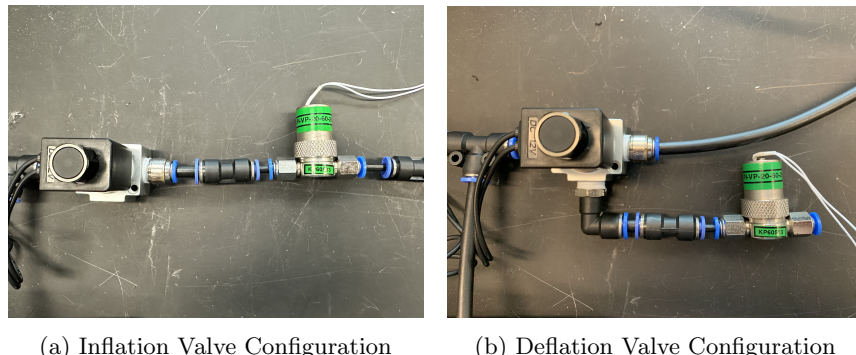


Fig. 1: Real-time length sensing test rig. The extruded aluminum frame holds a sliding crossbeam that displaces as an attached 180 cm long, 10mm diameter stock Festo BPA is inflated and deflated with two respective inflation and deflation configurations of a binary solenoid valve and a proportional valve. A linear potentiometer collects precise experimental length measurements for comparison with the Liquid Wire strain gauge sensor.



(a) Inflation Valve Configuration (b) Deflation Valve Configuration

Fig. 2: Valve configurations to regulate muscle inflation (a) and muscle deflation (b). This was done to account for sensor strain rate and hysteresis.

of muscle inflation and deflation rate to better characterize sensor strain rate and hysteresis.

A P3 America LMC13 linear motion potentiometer collected precise experimental length measurements for comparison with the Liquid Wire flexible strain gauge sensor.

2.1 Liquid Wire Strain Gauge Sensor

This study explores the application of flexible strain gauge sensors developed by Liquid Wire in Portland, Oregon [7] for use in biomimetic research. These sensors consist of channels within Thermoplastic Polyurethane (TPU) filled with a proprietary Gallium-Indium-Tin Metal Gel TM, as depicted in Figure 3. The selected TPU exhibits high elasticity, supporting over 30 percent strain, and demonstrates rapid recovery capabilities that contribute to reduced hysteresis. The Metal Gel TM is a shear-thinning gel featuring specifically engineered cross-linked oxide structures [11]. This composition provides a dual nature—solid yet flowable—enabling the gel to stretch with the material, thereby linearly increasing resistance as it extends the conductive path. Upon retraction, the gel returns to its original shape, effectively maintaining low hysteresis with the TPU.

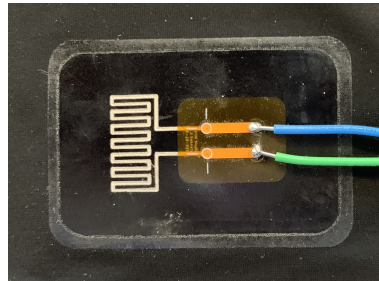


Fig. 3: Liquid Wire flexible strain gauge sensor consisting of channels within Thermoplastic Polyurethane filled with a proprietary Gallium-Indium-Tin Metal Gel TM.

2.2 Strain Gauge Application Method

The priorities in determining an application method for attaching the Liquid Wire sensor to the BPA were durability, modularity, biomimicry, and a low profile. The method that proved most successful and was ultimately pursued was heat-pressing the sensor onto nylon fabric and sewing the fabric into a flexible, modular cuff that could be mounted onto the BPA, with the strain gauge parallel to the displacement of the muscle, as seen in Figure 4. This method satisfied the desired design priorities, making it suitable for BPA soft-robotics applications.

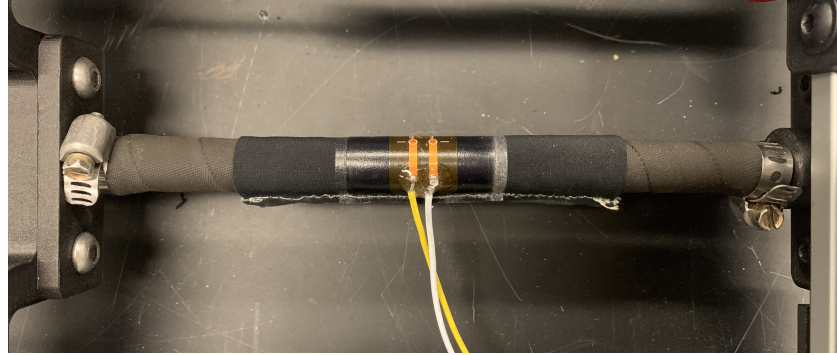


Fig. 4: Flexible Strain Gauge Sensor Sewn Sleeve

2.3 Circuitry

The strain gauge sensor was installed in a quarter Wheatstone bridge configuration, using a Spectrol 70Y-100 trimming potentiometer to balance the bridge and an INA125 instrumentation amplifier to amplify the signal by a gain of 10 for reading on an Arduino Due. A bridge input voltage over 1.5V resulted in drift of the strain gauge signal, so this voltage was kept below 1.5V. As mentioned, a separate P3 America LMC13 linear motion potentiometer was used as a true length measurement for comparing to the strain gauge signal. It was calibrated by using a tape measure to measure the muscle length at its inflated and deflated states and using those measured values to linearly interpolate. The proportional valve was configured using a current driver circuit and controlled using a PWM signal [2].

2.4 Actuation Trials

In order to examine the effect of strain rate and hysteresis on the characterization of the Liquid Wire sensor, displacement from the potentiometer and amplified change in voltage across the wheatstone bridge were sampled at 100Hz for six muscle inflation and deflation rates. For the inflation trials, the inflation valve configuration from Figure 2 was used to modulate the flow of air into the muscle by adjusting the proportional valve PWM value to change the inlet cross-sectional area. For the six trials, PWM values corresponding to a 0.25, 12.5, 25, 50, 75, and 100 percent open cross-sectional inlet area were used. For the deflation trials, the deflation valve configuration from Figure 2 was used to control the flow of air out of the muscle by similarly calling PWM values corresponding to a 0.25, 12.5, 25, 50, 75, and 100 percent cross-sectional outlet area. These two valve configurations were necessary due to the proportional valve not being able to control both inflation and deflation within the same trial.

To later validate the effectiveness of the flexible strain gauge attachment and calibration methods, two trials were conducted actuating the BPA, one where

the BPA was inflated and deflated arbitrarily at a range of strain rates and the other using repeating pulses to simulate neuron firing as a more biomimetic method of BPA actuation. The pulses used in these trials were two sequential pulses with a consistently decreasing pulse gap to investigate the effect of the pulse gap on the strain gauge sensor accuracy.

2.5 Data Processing and Strain Gauge Calibration

To characterize the flexible strain gauge, two calibration methods were pursued: one two-dimensional linear fit that does not account for hysteresis and strain rate and one three-dimensional non-linear fit that does. For the two-dimensional linear fit, the potentiometer displacement values were converted to strain, then the values for strain and voltage across the wheatstone bridge were both normalized by their total ranges. Normalized strain was plotted against normalized voltage for all inflation and deflation data sets and a linear best fit equation was generated using MATLAB, taking voltage as an input and generating strain as an output. The calibration equation was generated using normalized values to facilitate visualizing the relationships between the different variables and to standardize the equation for future use. To examine the success of the linear calibration method, the collected strain gauge voltage data from both the arbitrary actuation trial and the repeating pulse trial were normalized by their total ranges and inputted into the linear calibration equation to yield normalized strain as an output. This normalized strain was converted to represent displacement of the muscle in millimeters and was plotted against the potentiometer displacement data. Average error between the strain gauge displacement calculation and the potentiometer displacement data was calculated using the equation below:

$$err = \frac{(d_p - d_s)}{\delta} \cdot 100$$

where err is percent error, d_p is the potentiometer displacement signal, d_s is the strain gauge displacement signal, and δ is the range of the strain gauge displacement values. Root mean squared error was calculated using the following equation:

$$RMSE = \sqrt{\frac{1}{n} \cdot \sum_{i=1}^n (d_p - d_s)^2}$$

where n is the number of data points in the set.

For the three-dimensional non-linear fit, the potentiometer displacement values were converted to strain, the strain was then differentiated over time to yield instantaneous strain rate, and strain, strain rate, and voltage were all normalized by their total ranges. First, all inflation trials were plotted on a three-dimensional plot with normalized strain rate as the x-axis, normalized voltage as the y-axis, and normalized strain as the z-axis. A polynomial fit was generated in the MATLAB curve fitting tool with one degree in the x-axis and three degrees in the y-axis. This fit acted as the strain gauge non-linear inflation calibration equation,

taking normalized strain rate and bridge voltage as inputs and generating normalized strain as an output. Second, the plotting and curve fitting was repeated for the deflation trials, producing a similar strain gauge non-linear calibration equation for muscle deflation. To examine the success of the non-linear calibration method for real-time BPA actuation, the collected strain gauge voltage data from both the arbitrary actuation trial and the repeating pulse trial were first normalized by dividing by their total ranges. Instantaneous voltage rate was calculated by differentiating strain gauge voltage over time. Voltage rate was then normalized by dividing by its total range. Using normalized voltage and voltage rate as inputs, the non-linear inflation and deflation calibration equations were used to produce normalized strain as the output. This normalized strain was redimensionalized to represent displacement of the muscle in millimeters and was superimposed with the potentiometer displacement data. Average error and root mean squared error were calculated using the same equations as above.

3 Results

A Liquid Wire flexible strain gauge sensor, ironed onto a Nylon sleeve and mounted to an artificial BPA muscle, was used as a means of measuring real-time displacement. Figure 5 shows raw data from the strain gauge and potentiometer for the arbitrary actuation trial (top) and repeated pulse trial (bottom). For the arbitrary actuation trial, the calculated average percent error was 14.10 percent and the RMSE was 2.169 percent normalized strain. For the repeated pulse trial, the calculated average percent error was 5.180 percent and the RMSE was 0.9266 percent normalized strain. It can be seen that the strain gauge roughly follows the potentiometer displacement reading, though it exhibits considerable noise, irregular behavior, and delay.

From here, two methods of calibration were considered: a linear calibration that excludes strain rate and hysteresis and a non-linear calibration that considers inflation or deflation of the muscle and accounts for strain rate.

3.1 Linear Calibration

The relationship between muscle strain, as calculated by the potentiometer, and the voltage across the Wheatstone bridge can be seen in Figure 6.

A linear approximation was fit to this data as the simplest possible calibration and as a point of comparison, even though clear non-linearities can be seen. The best fit linear approximation equation was found to be

$$\varepsilon = 0.9744 \cdot V + 0.1757$$

and had a r^2 value of 0.9680.

3.2 Non-Linear Calibration

For the non-linear calibration, two separate calibrations equations were generated, one for inflation and one for deflation. To generate the inflation and deflation calibration equations, three-dimensional plots were generated with strain

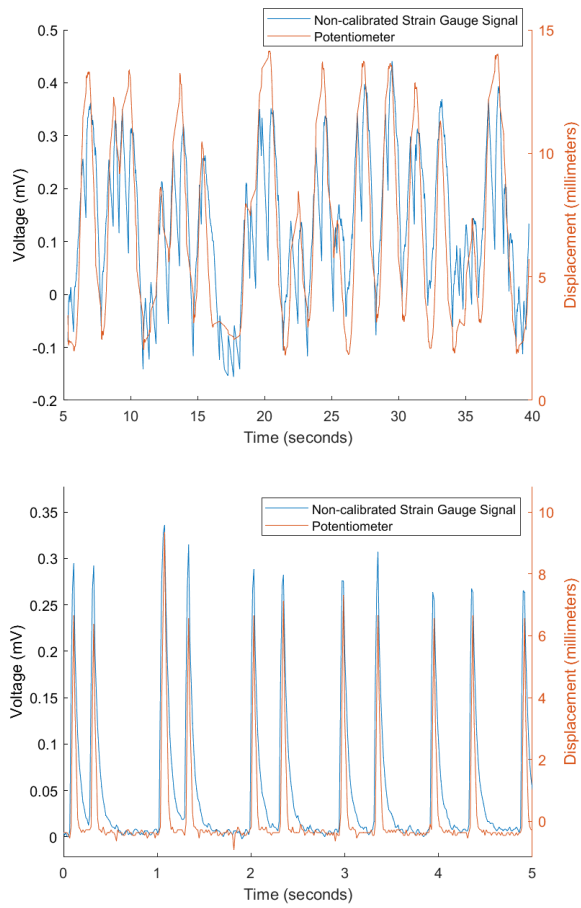


Fig. 5: Liquid Wire sensor reading pre-calibration for random actuation (top) and pulse based actuation (bottom)

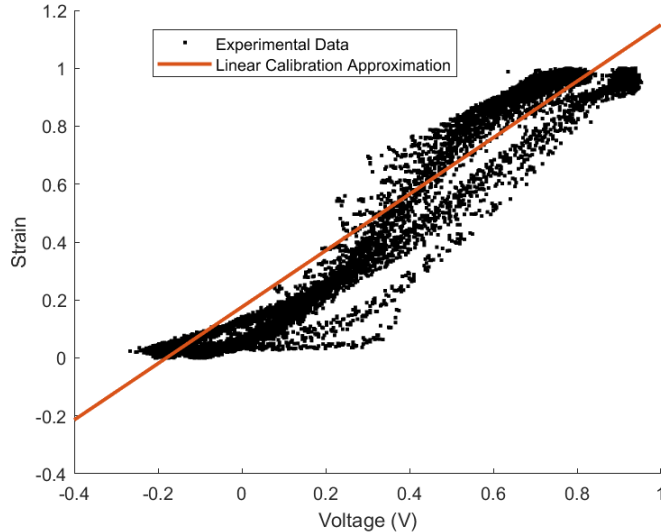


Fig. 6: Strain vs. voltage data and accompanying linear calibration approximation

rate as the x-axis, bridge voltage as the y-axis, and strain as the z-axis. A polynomial best fit of one degree in the x-axis and three degrees in the y-axis was generated as the non-linear calibration equation for each curve. The inflation and deflation calibration curves can be seen in Figure 7.

The corresponding best fit equation for inflation is:

$$\varepsilon = 0.058 + 0.001 \cdot \dot{\varepsilon} + 0.774 \cdot V - 0.121 \cdot V \cdot \dot{\varepsilon} + 2.30 \cdot V^2 + 0.094 \cdot \dot{\varepsilon} \cdot V^2 - 2.26 \cdot V^3$$

where $\dot{\varepsilon}$ is equal to strain rate, V is voltage across the wheatstone bridge, and ε is strain. The R^2 value for the fit is 0.9934 and the RMSE is 2.851 percent normalized strain. This fit was chosen because it was the lowest order fit that produced an impactful R^2 value, with the next lowest order fit having an R^2 value of 0.9806 and an RMSE of 4.890 percent normalized strain, while the next highest order fit had an R^2 value of 0.9938 and an RMSE of 2.765 percent normalized strain.

The corresponding best fit equation for deflation is:

$$\varepsilon = 0.225 - 0.218 \cdot \dot{\varepsilon} + 0.825 \cdot V - 0.773 \cdot V \cdot \dot{\varepsilon} - 0.481 \cdot V^2 + 1.05 \cdot \dot{\varepsilon} \cdot V^2 + 0.564 \cdot V^3$$

The R^2 value for the fit is 0.9943 and the RMSE is 1.821 percent normalized strain. This fit was chosen because it was the lowest order fit that produced an impactful R^2 value, with the next lowest order fit having an R^2 value of 0.9895 and an RMSE of 2.467 percent normalized strain, while the next highest order fit had an R^2 value of 0.9945 and an RMSE of 1.798 percent normalized strain.

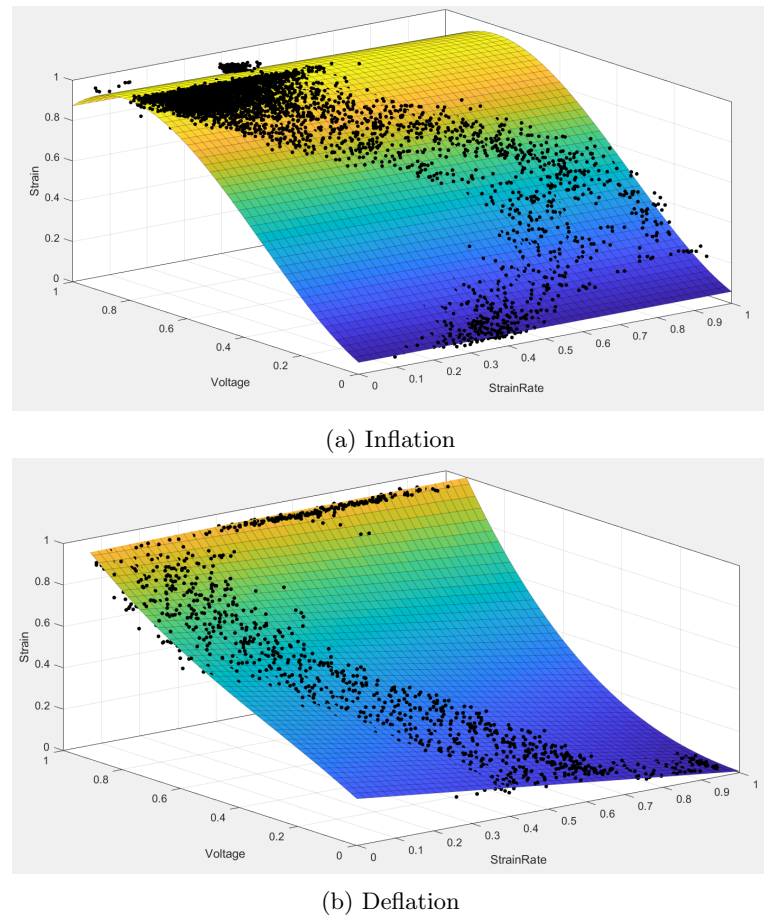


Fig. 7: Non-Linear Calibration Curves

3.3 Applied Linear Calibration

The results of applying the linear calibration equation show an average error of 18.62 percent and an RMSE of 3.807 percent normalized strain for the random actuation data and an average error of 5.875 percent and an RMSE of 1.845 percent normalized strain for the pulse data, as seen in Figure 8.

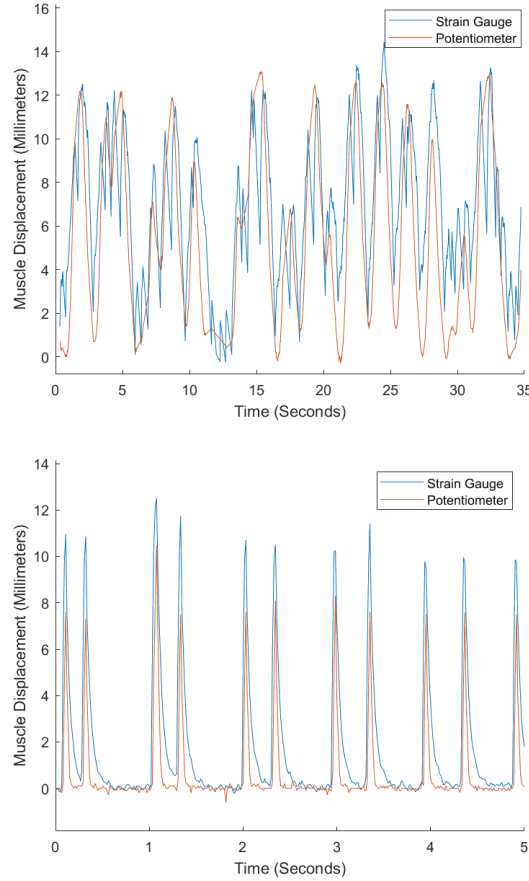


Fig. 8: Linearly calibrated random actuation (top) and pulse based actuation (bottom)

In the random actuation trials, the strain gauge signal exhibits a similar amount of noise as the raw data and does not reach the full magnitude of the potentiometer length reading. The pulsing actuation trials show minimal error in the strain gauge sensor reading but does demonstrate some delay and overshoot in comparison to the potentiometer signal.

3.4 Applied Non-Linear Calibration

The results of applying the non-linear calibration equations show an average error of 16.05 percent and an RMSE of 2.777 percent normalized strain for the random actuation data and an average error of 4.863 percent and an RMSE of 1.550 percent normalized strain for the pulse data, as seen in Figure 9.

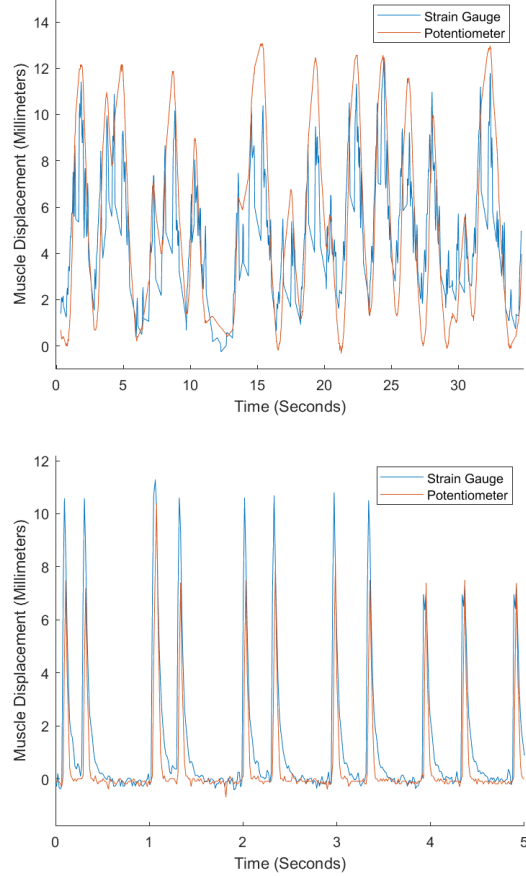


Fig. 9: Non-Linearly calibrated random actuation (top) and pulse based actuation (bottom)

The non-linearly calibrated strain gauge signal demonstrates a comparable amount of noise to the raw data and similarly to the linear calibration, the strain gauge signal does not reach the full magnitude of the potentiometer length reading. The non-linear calibration appears to perform well in the pulse-based actuation trials, though also shows some delay and overshoot in comparison to

the potentiometer signal. In comparison with the linearly-calibrated signal, the non-linearly calibrated signal exhibits less overshoot of the potentiometer signal.

4 Discussion

This research examines the validity of using Liquid Wire flexible strain gauges as a means for measuring real-time length feedback of BPA artificial muscles. The success of the proposed methods is highlighted by the modularity and consistency of the sensor sleeve, the low-profile and biomimetic nature of the strain gauge sensor, and the performance of two calibration methods—one linear calibration that neglects strain rate and hysteresis and one non-linear calibration that does not. The clear victory in the methods is seen especially in quantifying the pulse-based actuation, where for both calibration methods, the strain gauge signal exhibits low average percent error and low RMSE. The two methods are nearly interchangeable for this trial due to their similar error values, though the non-linear calibration does outperform the linear calibration and provides a higher level of accuracy. A paired T-test examining the two methods in the pulse-based actuation trials revealed a two-tailed P-value of less than 0.0001, demonstrating that this difference can be considered extremely statistically significant. Overall, the performance of the proposed methods in the pulse-based actuation trials demonstrates a two-fold biomimetic success: a low-profile and flexible real-time BPA length sensor that mimics the function of muscle stretch receptors, especially for pulse-based BPA actuation that simulates neuron firing for muscle activation.

The low average error and RMSE in the pulse-based actuation trials could be due to the periods of rest between the pulses. The displacement of the muscle during these periods is very low, ultimately decreasing the overall average error and RMSE. This prompts further examination of the relationship between pulse width and strain gauge sensor accuracy, where generally within this trial, the success of the strain gauge was unaffected. In comparison with the non-calibrated signal, low significant improvement was made using either calibration method and further analysis is required to determine the impact of the calibration equations for pulse-based actuation. Ultimately, a better understanding of the success of these methods could be achieved through more thorough characterization of sensor responses and understanding of the frequency response. Further analysis of the voltage rate should equally be investigated, especially in conjunction with pulse-based actuation pulse width.

While the linear and non-linear calibration methods vary slightly in their successes for the pulse-based actuation, both methods equally failed to outperform the non-calibrated strain gauge signal for the random actuation trial. It is hypothesized that the higher frequency of rapid changes in direction and inflation rate produced more error for this trial. This high error warrants pursuing signal filtering in future work to further investigate the application of the flexible strain gauges and proposed calibration methods in random BPA muscle actuation.

In comparison to a similar experiment that examines the impact of strain rate and hysteresis on piezoresistive real-time BPA length sensing, the methods proposed in this work demonstrate a similar success in random BPA actuation. In the study, the found RMSE value for the proposed piezoresistive flexible sensor signal was 1.27 mm, about 20 percent of entire axial displacement of the actuator [9]. While the methods proposed vary in their sensor construction, the similarities between their sensor characterization methods provide an opportunity to compare their results. Overall, the measured error in the Liquid Wire flexible strain gauge signal is slightly lower than in the proposed piezoresistive flexible sensor, potentially highlighting the high elasticity, and therefore generally low hysteresis, of the Liquid Wire sensor. Ultimately, this research shows that using Liquid Wire flexible strain gauges for real-time BPA length-sensing highlights a unique application of this genre of sensor: measuring pulse-based BPA actuation.

5 Acknowledgements

This work could not have been accomplished without the help of Connor Blanckenuau and Ben Bolen. Partially-funded by NSF grant for NeuroNex: C3NS 2015317.

6 Disclosure of Interests

Author Michael Hopkins is an employee of Liquid Wire.

References

1. Antonelli, M.G., Zobel, P.B., De Marcellis, A., Palange, E.: Design and characterization of a mckibben pneumatic muscle prototype with an embedded capacitive length transducer. *Machines* (2022)
2. Chakravarthy, S., Kapilavai, A., Ghosal, A.: Experimental characterization and control of miniaturized pneumatic artificial muscle. *Journal of Medical Devices* (2014)
3. Chung, J.: Real-time length sensing of braided pneumatic actuator using ir time-of-flight sensor (2023)
4. Dai, K., Elangovan, A., Whirley, K., Webster-Wood, V.A.: Soft tubular sensors for contact detection. 12th International Conference, Living Machines 2023, Proceedings, Part I (2023)
5. Felt, W., Chin, K.Y., Remy, D.: Contraction sensing with smart braid mckibben muscles. *IEEE/ASME Transactions on Mechatronics* (2015)
6. Goulbourne, N.C., Son, S.: Numerical and experimental analysis of mckibben actuators and dielectric elastomer sensors. *ASME 2007 International Mechanical Engineering Congress and Exposition* (2009)
7. [Https://www.liquidwire.com/](https://www.liquidwire.com/), Accessed: 2024-04-12
8. Jankowska, E.: Spinal interneuronal networks in the cat: Elementary components. *Brain Research Reviews*, Networks in Motion, 57, no. 1: 46–55 (2008)

9. Maselli, M., Zrinscak, D., Magliola, V., Cianchetti, M.: A piezoresistive flexible sensor to detect soft actuator deformation. 2019 2nd IEEE International Conference on Soft Robotics (RoboSoft) (2019)
10. Prochazka, A.: Quantifying proprioception. *Progress in Brain Research* 123: 133–42 (1999)
11. Ronay, M.: (2017), wO2017151523A1
12. Wakimoto, S., Suzumori, K., Kanda, T.: Development of intelligent mckibben actuator. *IEEE/RSJ International Conference on Intelligent Robots and Systems (IROS)* (2005)
13. Wirekoh, J., Valle, L., Pol, N., Park, Y.L.: Sensorized, flat, pneumatic artificial muscle embedded with biomimetic microfluidic sensors for proprioceptive feedback. *Soft Robotics* (2019)